Supplementary Information

Nucleation of Decahedral Ag Nanoclusters

*Yi-Kang Lan, Chiu-Hun Su, Wen-Hsien Sun, and An-Chung Su**

MD Protocol

Commercial package *Accelrys® Materials Studio* was used for geometry optimization and MD simulation engines (*Forcite*). Considerations for a further study (not reported here) of polymer/cluster interactions, COMPASS force field was chosen for the followed heating, isothermal and coalescence MD simulations. All the MD computations were made with COMPASS force field, the Verlet integrator, NVT ensemble and 1.25 nm cut-off distance. The Nose method was adopted for the thermostat. Partial charges of silver atoms were set from the COMPASS parameter. Time steps of 0.1 fs were chosen during coalescence MD for more detailed observations; otherwise time steps of 1 fs were used.

MD Algorithm

The Verlet velocity algorithm overcomes the out-of-synchrony shortcoming of the Verlet leapfrog method. The Verlet velocity algorithm is as follows:

$$r(t+\Delta t) = r(t) + \Delta t\, v(t) + \frac{\Delta t^2\, a(t)}{2}$$

$$a(t+\Delta t) = \frac{f(t+\Delta t)}{m}$$

$$v(t+\Delta t) = v(t) + \frac{1}{2}\Delta t\,[a(t) + a(t+\Delta t)]$$

where **r**(*t*), **v**(*t*), and **a**(*t*) are respectively the position, velocity, and acceleration at time *t*.

Forcefield Parameters

COMPASS is an *ab initio* forcefield, which the most parameters were derived based on *ab initio* data. The potential form of COMPASS is given as

$$E_{COMPASS} = \sum_b \left[K_2(b-b_0)^2 + K_3(b-b_0)^3 + K_4(b-b_0)^4\right] + \sum_\theta \left[H_2(\theta-\theta_0)^2 + H_3(\theta-\theta_0)^3 + H_4(\theta-\theta_0)^4\right] + \sum_\phi \left[V_1\left[1 - cos(\phi -\right.\right.$$

where the first 4 terms in the CFF forcefield family involve the quadratic polynomials for bond stretching and bending, a three-term Fourier expansion for torsions and the out-of-plane/inversion. Terms 5 to 11 are cross-terms up to the third order that have been found to be important. Terms 12 and 13 represent non-bonded terms with the Coulombic interaction between the atomic charges and the van der Waals interactions. In addition to this, COMPASS supports the Morse-dispersion form (Term 14) that appears in semi-ionic models, typically used in the simulation of metal oxide systems.

Table S1. List of the delay time τ between the pre-transitional (first) step and the major (second) step of the Dh→Ih transformation obtained with the isothermal MD at various temperatures. For each temperature, 3 MD runs were performed to give the averaged τ.

T (K)	200	225	250	275	300	325
1st Run	4.38E-09 s	2.52E-10 s	1.95E-10 s	7.40E-11 s	5.20E-11 s	1.40E-11 s
2nd Run	5.08E-09 s	8.37E-10 s	4.56E-10 s	1.12E-10 s	2.80E-11 s	1.35E-11 s
3rd Run	1.70E-09 s	6.96E-10 s	4.82E-10 s	6.20E-11 s	3.71E-11 s	1.35E-11 s
⟨τ⟩	3.72E-09 s	5.95E-10 s	3.77E-10 s	8.28E-11 s	3.90E-11 s	1.37E-11 s

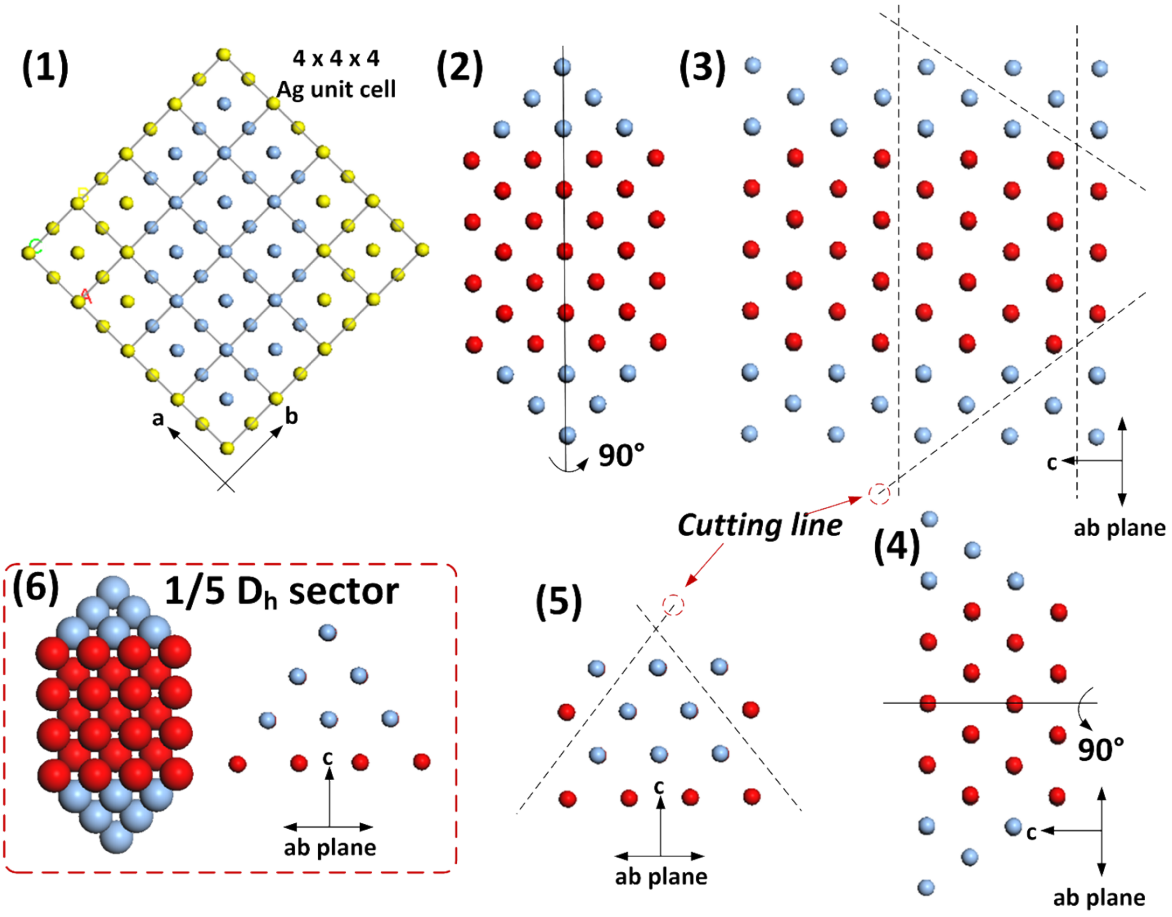

Figure S1. Generation of Dh clusters. (1) Prepare an FCC crystal of 4 × 4 × 4 unit cells and delete the selected rows (colored in yellow) along the *c*-axis. (2) Turn the structure by 90°. (3) Delete the rows outside the cutting lines to result in (4), followed by another 90°-rotation and deletion of rows as shown in (5). Given in (6) is one of the 5 sectors of the Dh cluster with $S = m = n = 4$. Finally, duplicate the sector and combined these to form the complete Dh cluster. If one needs to build a sequence of clusters of different sizes, the simplest way is to build the biggest cluster first, then delete the outer shells to obtain smaller clusters.

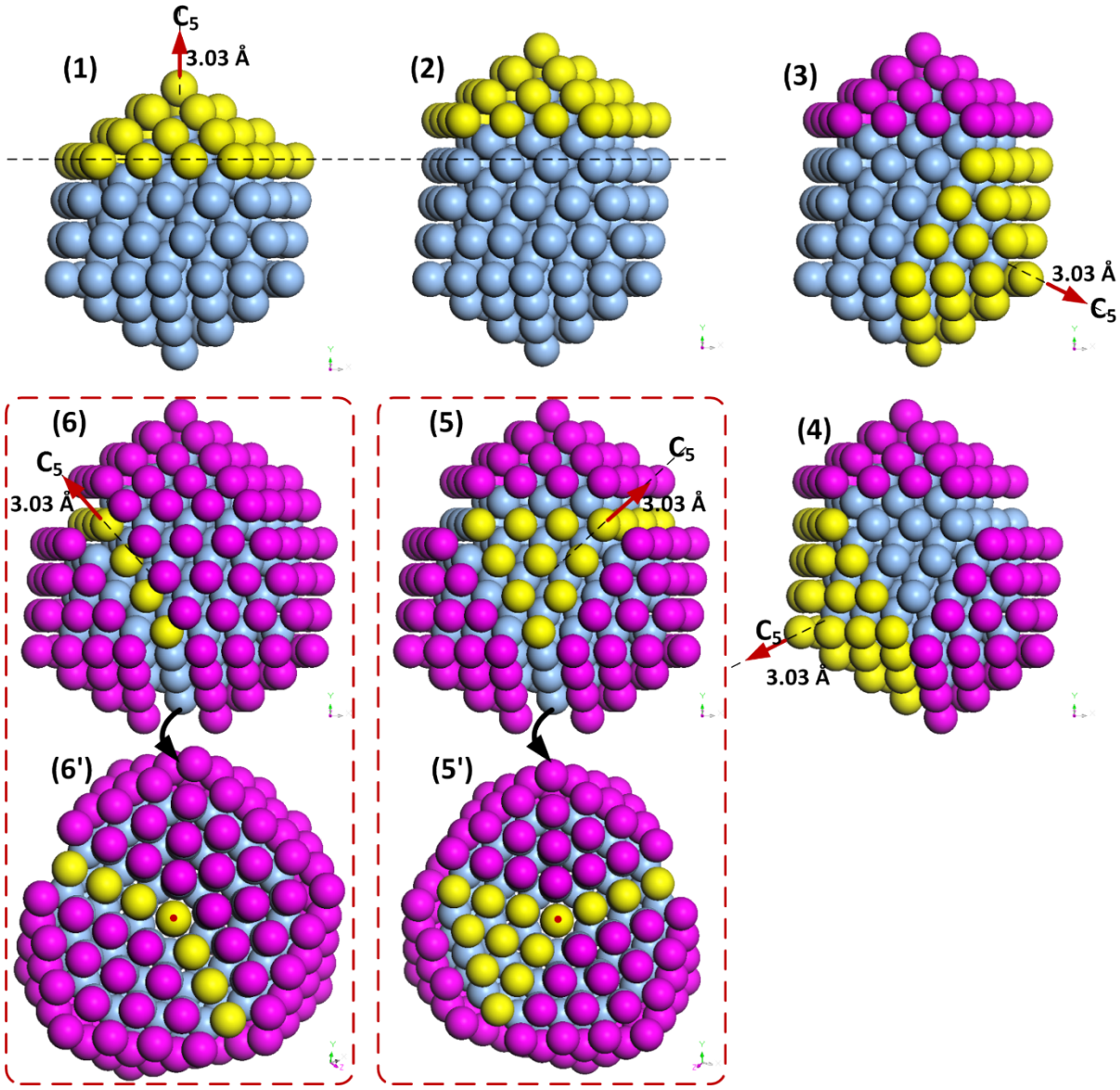

Figure S2. Generation of Ih clusters. An Ih cluster is hard to build because of its off-FCC packing. Here we demonstrate a way to generate the cluster layer by layer. The initiating structure is based on a small Ih cluster such as N_4, which can be obtained via MD-simulated transformation from the corresponding Dh cluster. (1) Based on the initial N_4 cluster of Ih symmetry, duplicate (as yellow atoms) the upper cap of the top pyramid. (2) Displace the newly generated atoms by 3.03Å along the C_5-axis. This procedure is repeated in (3) to (6) until a new surface shell is generated. After geometry optimization, the one-shell-added Ih cluster is obtained and ready for subsequent generation of larger clusters.

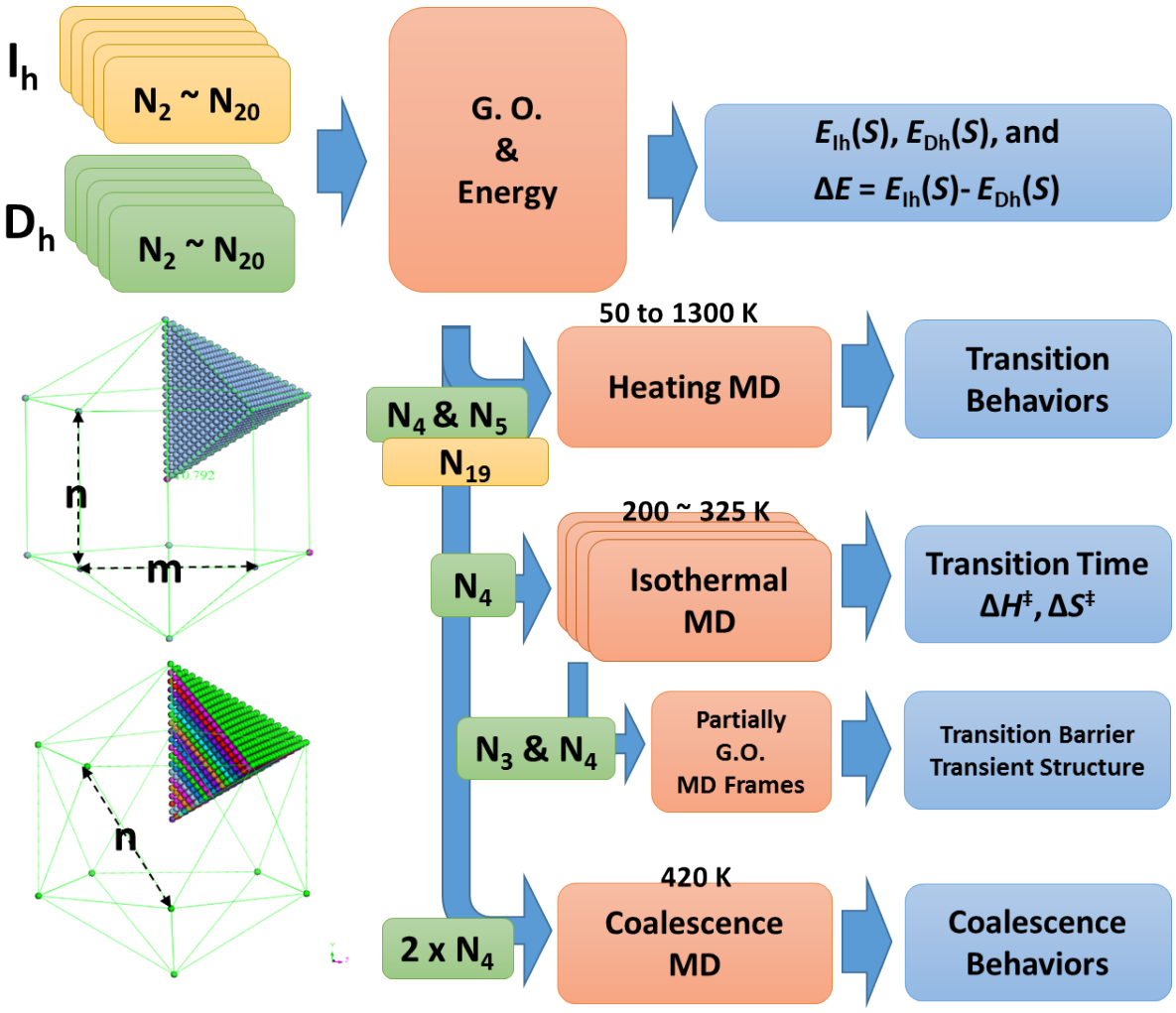

Figure S3. Strategy of computation. After fully geometry optimizations applied to the sequence of Ih and Dh clusters ranging from N_2 to N_{20} in size, the total potential energy of each cluster (E) was calculated. Two Dh clusters (N_4 and N_5) and one Ih cluster (N_{19}) were chosen for "heating" MD simulation to identify the corresponding transformation temperature ($T_{\text{Ih-Dh}}$) between Ih and Dh forms. The heating rate was set to 10^{-2} K/ps for the N_4 cluster from 50 to 250 K, 10^{-3} K/ps for the N_5 cluster from 100 to 1100 K, and 0.2 K/ps for the N_{19} cluster from 300 to 1300 K, respectively. With $T_{\text{Ih-Dh}}$ estimated, isothermal MD calculations of the N_4 system were performed at 200 K to 325 K (in 25 K intervals) to obtain Eyring parameters $\Delta H^{\ddagger}$ and $\Delta S^{\ddagger}$. Furthermore, MD simulation at 300 K for N_4 and 90 K for N_3 were repeated with finer time steps of 0.1 fs, with MD frames in the trajectory partially minimized by steepest-descent method for 100 iterations to trace the changes in the transient structure. Finally, two N_4 clusters with 20 Å separation were set at 420 K to examine the cluster coalescence process.

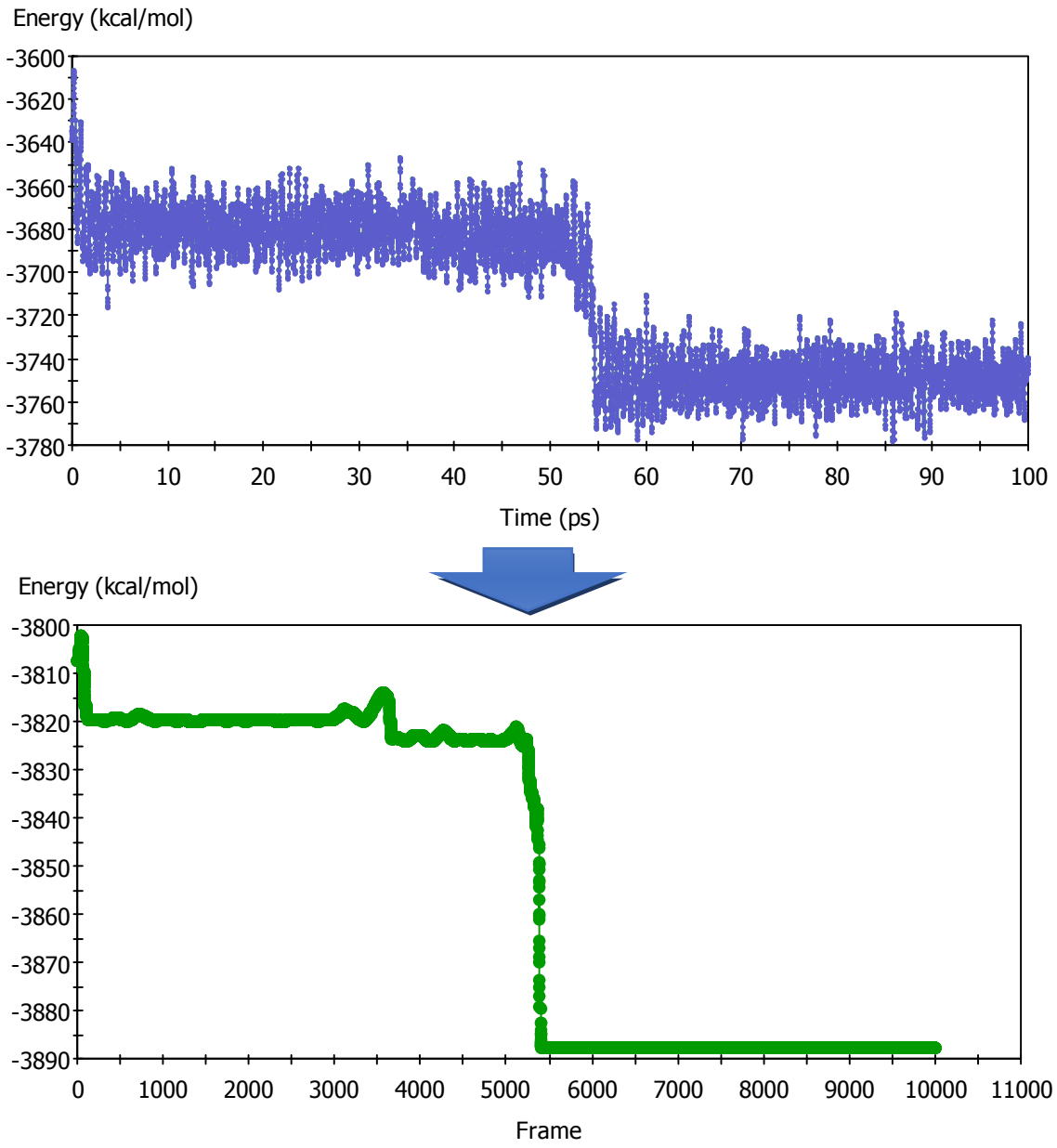

Figure S4. Partial geometry-optimization via steepest descents. To eliminate the fluctuation in the MD trajectory and find out the transient structure evolution, an MD run at 300K was chosen to be repeated with shorter time steps of 0.1 fs to catch the evolution details. All 10^5 frames (100 differential steps between frames) were optimized with the steepest-descent method. In the steepest descents method, the line search direction is defined along the direction of the local downhill gradient and each line search produces a new direction that is perpendicular to the previous gradient; however, the directions oscillate along the way to the minimum. This inefficient convergence is characteristic of the steepest-descent method, especially on energy surfaces with narrow valleys. The exclusive reliance on the local gradient is both its weakness and its strength. Convergence is slow near the minimum because the gradient approaches zero; on the other hand, the method is extremely robust, even for far-from-harmonic systems. Therefore, a few iterations of the steepest-descent method provide partially stabilized, incompletely converged transient structures along the MD trajectory.

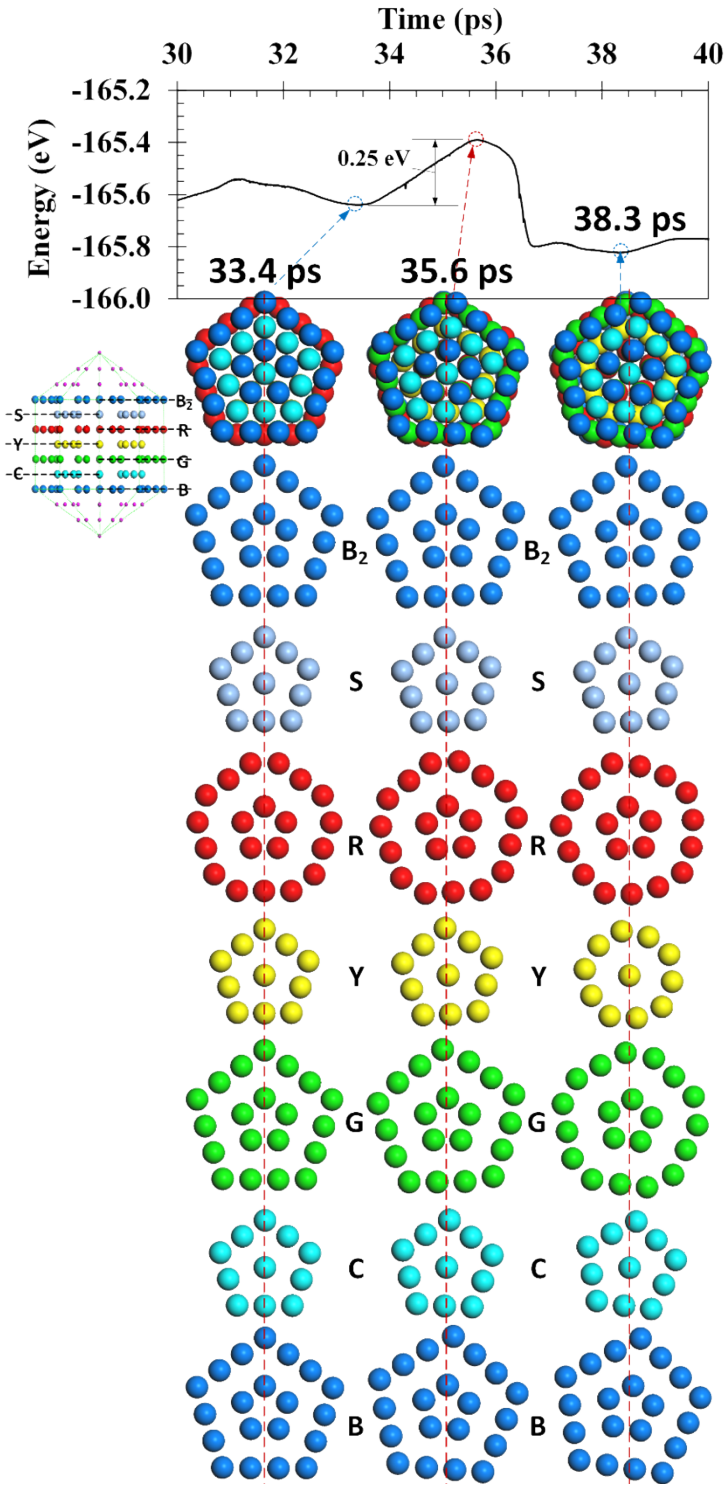

Figure S5. Details of the key ("second") step-change in the Dh→Ih potential energy evolution profile along the partially geometry-optimized MD trajectory of an N_4 cluster at 300 K. Three representative transient structures and corresponding changes in atomic positions of each cross-sectional layer are also demonstrated. Atoms in the "stem" between the two pentagonal pyramids at upper and lower ends of the original Dh cluster are colored in the sequence of blue (B_2), silver (S), red (R), yellow (Y), green (G), cyan (C), and blue (B). The barrier of ca. 0.25 eV between transient structures at t_{MD} = 33 and 36 ps corresponded mainly to coordinated rotation of atoms in the C/B double-deck (for which the periphral atoms experience little friction). This was then followed by transformation to Ih geometry with minor aomic repositioning in the Y/G layers, further clockwise rotation of the B/C layers, and slight rotation of peripheral atoms in the S layer.

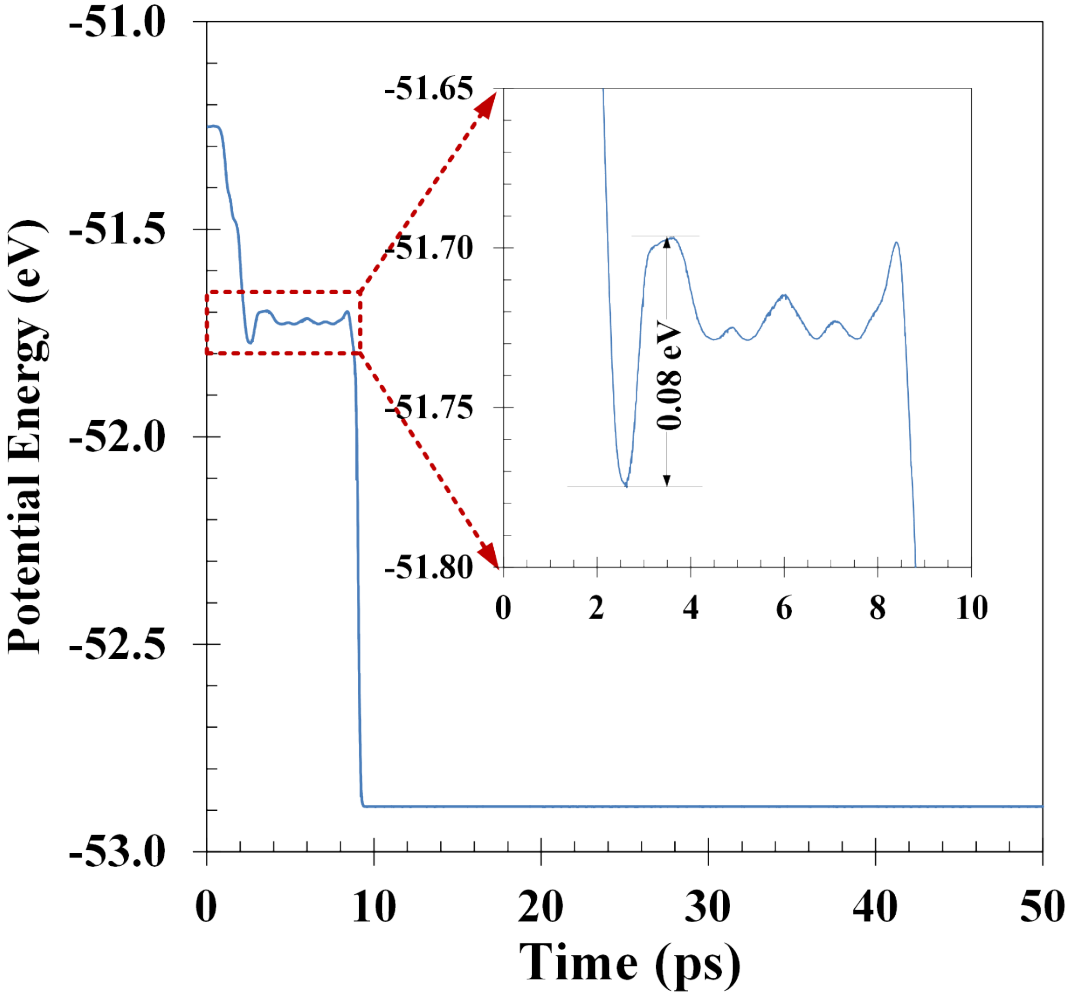

Figure S6. Potential energy evolution profile along the partially geometry-optimized MD trajectory of an N_3 cluster at 90 K, starting from the energetically unfavorable Dh form. Partial GO was made to each MD frame (in 10 fs intervals) with the speedest-descent method for 100 steps. The inset is a magnified view to demostrate the first quick drop for a transient minimum at $t_{MD} \approx 2.5$ ps, followed by surpassing a barrier of 0.08 eV for a higher-energy plateau before the second step drop in energy at $t_{MD} \approx 9$ ps to reach the stable Ih form.